Improved modified-moment-singularity method

Michael G. Prais* and John C. Wheeler
Chemistry Department, B-014, University of California, San Diego, La Jolla, California 92093
(Received 10 September 1985)

Improvements are made in the moment-singularity method for the calculation of densities of state in the vicinity of van Hove singularities using modified moments by simplifying the functional form of the singular behavior that is used to fit the densities. Because the asymptotic behavior of the modified moments determines and is determined by the singular behavior of the density, information about the locations and functional forms of the singularities can be determined directly from the moments themselves and incorporated into the calculation of the density. The use of simplified functional forms to fit the singular behavior facilitates the use of the higher-order (less singular) corrections to the dominant singular behavior. These higher-order corrections to the singular behavior improve the precision to which the locations of the singularities can be determined and the precision to which the exact densities can be fit. The use of simplified functional forms also facilitates the treatment of singularities at the ends of the interval and within band gaps. This is advantageous in the reconstruction of densities whose behavior at the ends of the interval is not fit well by the Chebyshev weight function. The moment-singularity method is illustrated with applications to three different densities of states: (1) the density of a linear diatomic chain with $m/M=\frac{1}{2}$, (2) the average of the densities of two diatomic chains, one word with $m/M=\frac{1}{2}$ and the other with $m/M=\frac{1}{5}$, and (3) the density of the two-dimensional triangular lattice with nearest-neighbor interactions. The precision of the moment-singularity method is also compared to that of the method of Corcoran and Langhoff for the reconstruction of densities.

I. INTRODUCTION

This paper describes improvements that can be made to the *moment-singularity* method which was originally proposed by Lax and Lebowitz[1] and Rosenstock[2] as a way of improving the precision of the moment method for the calculation of densities of states in the vicinity of van Hove singularities. This method takes into account the presence of known singularities by expressing the density of states as a sum of terms:

$$G(x)=G_s(x)+G_r(x)\ . \tag{1}$$

The first term describes the known singular behavior, which is usually the most singular behavior of the density and is represented by a sum of appropriate singular functions. The second term describes the remaining, less singular behavior of the density and is approximated by a (finite) sum over a set of orthogonal polynomials using the known moments. This method has been shown to be an improvement over the moment method when information about the location and nature of the singularities is known.

Wheeler, Prais, and Blumstein[3] (WPB) introduced an implementation of the moment-singularity method based on *modified moments*[4] in which information about the singularities can be obtained directly from the modified moments themselves and is then incorporated into the moment-singularity scheme. Wheeler and Blumstein[5] showed how these modified moments could be calculated by the same simple product-trace techniques used to calculate power moments. Using Chebyshev polynomials of the second kind, they expressed the density as a Fourier series in the transformed variable, $\theta=2\arcsin\sqrt{x}$:

$$G(x)=G(\sin^2(\theta/2))=(4/\pi)\sum_{n=0}^{\infty}\nu_n^*\sin(n+1)\theta\ , \tag{2}$$

where ν_n^* is the nth modified moment of $G(x)$ based on normalized Chebyshev polynomials of the second kind on the interval [0,1]. The singular behavior of the density can be separated from the rest using the modified moments because the asymptotic behavior of ν_n^* as $n\rightarrow\infty$ determines (and is determined by) the singular behavior of the density. Separating the asymptotic behavior from the modified moments leads to the following expression for the density:

$$G(\sin^2(\theta/2))=(4/\pi)\sum_{n=0}^{\infty}\nu_n^{*s}\sin(n+1)\theta +(4/\pi)\sum_{n=0}^{\infty}(\nu_n^*-\nu_n^{*s})\sin(n+1)\theta\ , \tag{3}$$

where ν_n^{*s} is a simple function of n that, for large n, possesses the asymptotic behavior required to reproduce the singularity and where the second sum is approximated with a finite sum using the known moments.

A class of singularities in the density that arises naturally in several areas of solid-state physics occurs when x (or, equivalently, θ) passes through an extreme value or saddle point as a function of one or more variables with respect to which the states are uniformly or smoothly distributed. Examples include van Hove singularities in the vibrational and electronic densities of states of solids. The asymptotic contributions to the nth modified moment from such a stationary point with a frequency given by θ_s have the form[6]

$$\nu_n^{*s} \sim A_s(n+1)^{-(p+1)}\sin[(n+1)\theta_s+\pi\epsilon_s/4] + B_s(n+1)^{-(p+2)}\sin[(n+1)\theta_s + \pi(\epsilon_s+2)/4]+\cdots , \quad (4)$$

where p is related to the spatial dimensionality d of the solid by $p=(d-2)/2$ and ϵ_s is a small integer that depends on the type of stationary point.

Wheeler, Prais, and Blumstein[3] observed that the first part of Eq. (3) could be summed exactly, using the expression in Eq. (4), to produce a known (although complicated) function, the behavior of which near $\theta=\theta_s$ could be expressed in terms of a closed-form nonanalytic piece and a rapidly convergent expansion with Riemann ζ functions as coefficients. With the most singular parts known exactly, the second part of Eq. (3) was approximated by a partial sum using the known moments. This moment-singularity method provides a very accurate determination of the density from relatively few moments. However, it suffers from the drawback that if higher-order corrections are employed or if singularities of several types are required, the complicated nature of the exact singular functions becomes burdensome.

In this paper we give an improvement on the WPB method based on a simplification of the functional form used to fit the singular behavior of the densities. This simplification is of considerable practical value in that it facilitates both the incorporation of higher-order (less singular) corrections to the dominant singular behavior and the treatment of singularities at the ends of the interval, while retaining the precision of the WPB method in determining the locations, types, and amplitudes of the singularities from the moments and in calculating the resulting densities. The use of higher-order corrections to the singular behavior is found to improve the agreement with the exact density and to improve the precision to which the locations of the singularities can be determined.

We have found this improved moment-singularity method very useful in analyzing and reconstructing densities for the motion of atoms near the surface of a solid.[7] Unusual types of van Hove singularities and modifications of the singular behavior at the ends of the interval make this technique especially valuable for that problem. Those results will be presented elsewhere. Here we describe the new method and illustrate its effectiveness by a comparison with earlier techniques. In Sec. II the improvements in the moment-singularity method are described. In Sec. III we apply this new method to three cases in which the exact densities are known and compare it to other approximation methods. These three cases—a linear diatomic chain, a superposition of two different linear diatomic chains, and a two-dimensional triangular lattice—provide densities with band gaps and with common singularities in the interior of the bands as well as at the band edges.

II. IMPROVED MOMENT-SINGULARITY METHOD

The singular behavior characteristic of odd-dimensional harmonic solids can be produced by the real part of the simple expression $A_s(1-e^{i\phi})^p$, namely,

$$\mathrm{Re}[A_s(1-e^{i\phi})^p] = |A_s|\,|2\sin(\phi/2)|^p\cos[\tfrac{1}{2}p(\phi-\pi\,\mathrm{sgn}\phi)-\pi\epsilon_s/4] , \quad (5)$$

where

$$A_s = |A_s|\exp(-i\pi\epsilon_s/4) .$$

When p is a half-integer and ϵ_s is an odd integer, the cosine in Eq. (5) will approach a nonzero constant from one side of the singular point and will approach zero from the other. Letting $\phi=\theta-\theta_s$, with $x=\sin^2(\theta/2)$ and $x_s=\sin^2(\theta_s/2)$, and using the expansion (for $x_s\neq 0,1$)

$$|2\sin(\phi/2)|^p = |x-x_s|^p[x_s(1-x_s)]^{-p/2}[1+O(x-x_s)] , \quad (6)$$

one sees that $p=-\frac{1}{2}$ in Eq. (5) produces a singularity of the type characteristic of one-dimensional harmonic solids and that $p=+\frac{1}{2}$ produces a singularity of the type characteristic of three-dimensional harmonic solids. In Figs. 1(a) and 1(b) we have plotted the singular functions calculated from Eq. (5) for $p=-\frac{1}{2}$ and $\epsilon_s=-1$ and for $p=+\frac{1}{2}$ and $\epsilon_s=+1$.

To get the moments associated with the singular functions in Eq. (5) the left-hand side of this equation can be expanded as

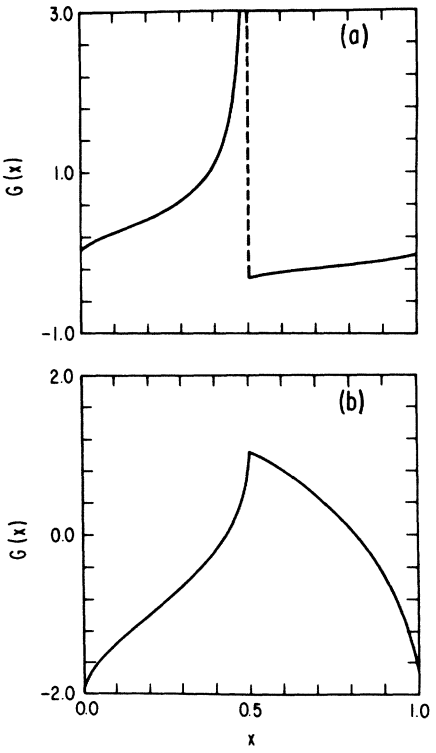

FIG. 1. Singular functions characteristic of (a) one-dimensional and (b) three-dimensional harmonic solids as obtained from Eq. (5) with $p=-\frac{1}{2}$ and ϵ_s-1 and with $p=+\frac{1}{2}$ and $\epsilon_s=+1$, respectively.

$$\mathrm{Re}[A_s(1-e^{i\phi})^p] = |A_s| \sum_{k=0}^{\infty} \frac{\Gamma(k-p)}{\Gamma(k+1)\Gamma(-p)} \cos(k\phi - \pi\epsilon_s/4) . \quad (7)$$

It is easy to see that singular behavior of the form

$$G_s(x) \sim (2/\pi)\mathrm{Re}[A_s(1-e^{i(\theta-\theta_s)})^p] - (2/\pi)\mathrm{Re}[\overline{A}_s(1-e^{i(\theta+\theta_s)})^p] \quad (8)$$

will be produced by using asymptotic contributions of the form

$$v_n^{*s} \equiv |A_s| \frac{\Gamma(n-p+1)}{\Gamma(n+2)\Gamma(-p)} \sin[(n+1)\theta_s + \pi\epsilon_s/4] \quad (9)$$

in Eq. (3). In Eq. (8), $\overline{A}$ is the complex conjugate of A. Only the singularity at $\theta = +\theta_s$ will appear in the density on the interval $0 \le x \le 1$, because we can choose θ to be in the interval $0 \le \theta \le \pi$. The asymptotic behavior of the ratio of gamma functions in Eq. (9) is, as $n \to \infty$,

$$\frac{\Gamma(n-p+1)}{\Gamma(n+2)\Gamma(-p)} \sim \frac{1}{(n+1)^{(p+1)}\Gamma(-p)} . \quad (10)$$

Thus, the asymptotic behavior of v_n^{*s} in Eq. (9) is equivalent to that in Eq. (4) for large n, but the moments in Eq. (9) produce a much simpler expression for the known singular behavior in the density than does the WPB method.

The singular behavior characteristic of even-dimensional harmonic solids cannot be deduced directly from the expression in Eq. (5) because it is analytic when p is a non-negative integer. However, the expression does have singular behavior near $p = m$ which can be seen from the expansion $p = m + \chi$ for small χ:

$$(1-e^{i\phi})^{m+\chi} = (1-e^{i\phi})^m [1 + \chi \ln(1-e^{i\phi}) + \cdots] . \quad (11)$$

The real part of the singular piece in this expression,

$$\mathrm{Re}[A_s(1-e^{i\phi})^m \ln(1-e^{i\phi})] = |A_s| \, |2\sin(\phi/2)|^m \{ \ln|2\sin(\phi/2)| \cos[\tfrac{1}{2}m(\phi - \pi\,\mathrm{sgn}\phi) - \pi\epsilon_s/4] - \tfrac{1}{2}(\phi - \pi\,\mathrm{sgn}\phi)\sin[\tfrac{1}{2}m(\phi - \pi\,\mathrm{sgn}\phi) - \pi\epsilon_s/4] \} , \quad (12)$$

where $A_s = |A_s| \exp(-i\pi\epsilon_s/4)$, will produce singular behavior at $\phi = 0$ of the type characteristic of even-dimensional harmonic solids. When m is a non-negative integer and ϵ_s is an even integer, one of the trigometric factors,

$$\cos[\tfrac{1}{2}m(\phi - \pi\,\mathrm{sgn}\phi) - \pi\epsilon_s/4]$$

or

$$\sin[\tfrac{1}{2}m(\phi - \pi\,\mathrm{sgn}\phi) - \pi\epsilon_s/4] ,$$

approaches a nonzero constant from both sides of the singular point. Using Eq. (6) in Eq. (12) one can recognize that the combination $m = 0$ and $\epsilon_s = 4$ produces a logarithmic divergence in the density that is characteristic of a saddle point in a two-dimensional Brillouin zone, while the combination $m = 0$ and $\epsilon_s = \pm 2$ produces the discontinuity associated with a two-dimensional maximum or minimum. In Figs. 2(a) and 2(b) we have plotted the singular functions calculated from Eq. (12) for $m = 0$ and $\epsilon_s = 4$ and for $m = 0$ and $\epsilon_s = -2$, respectively.

To determine the moments associated with the singular behavior in Eq. (12), the left-hand side of this equation can be expanded as

$$\mathrm{Re}[A_s(1-e^{i\phi})^m \ln(1-e^{i\phi})] = |A_s| \sum_{k=1}^{\infty} \left[\sum_{l=0}^{k-1} (-1)^{l+1} \binom{m}{l} \frac{1}{k-l} \right] \times \cos(k\phi - \pi\epsilon_s/4) , \quad (13)$$

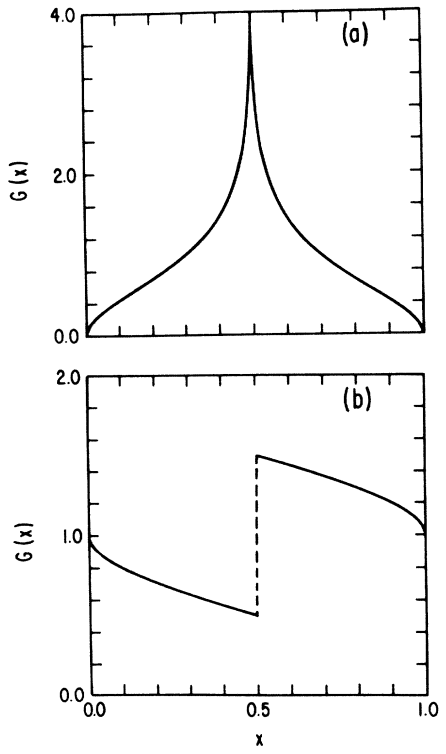

FIG. 2. (a) Logarithmic divergence and (b) discontinuity characteristic of two-dimensional solids as obtained from Eq. (12) with $m = 0$ and $\epsilon_s = 4$ and with $m = 0$ and $\epsilon_s = -2$, respectively.

where $\binom{m}{l}$ is the binomial coefficient $m!/[l!(m-l)!]$. It is easy to see that singular behavior of the form

$$G_s(x)\sim \frac{2}{\pi}\,\mathrm{Re}[A_s(1-e^{i(\theta-\theta_s)})^m \ln(1-e^{i(\theta-\theta_s)})] - \frac{2}{\pi}\,\mathrm{Re}[A_s(1-e^{i(\theta+\theta_s)})^m \ln(1-e^{i(\theta+\theta_s)})] \quad (14)$$

will be produced by using asymptotic moments of the form

$$\nu_n^{*s}= |A_s| \left\{ \sum_{l=0}^{n} \left[(-1)^{l+1} \binom{m}{l} \frac{1}{n-l+1} \right] \right\} \times \sin[(n+1)\theta_s+\pi\epsilon_s/4] \quad (15)$$

in Eq. (3). Because the binomial coefficient $\binom{m}{l}=m!/[l!(m-l)!]$ vanishes whenever $l>m$, the sum in Eq. (15) consists of, at most, $m+1$ terms. The maximum number of terms occurs when $m\le n$. In this situation the sum can be expressed as

$$\sum_{l=0}^{m}(-1)^l\binom{m}{l}\frac{1}{l-n-1} =(-1)^{m+1}\frac{\Gamma(m+1)\Gamma(n-m+1)}{\Gamma(n+2)} . \quad (16)$$

This simple expression can also be obtained from the expansion of the asymptotic moments in Eq. (9). Setting $p=m+\chi$ for small χ and with $n\ge m$, we have

$$\frac{\Gamma(n-p+1)}{\Gamma(n+2)\Gamma(-p)}=\frac{\Gamma(p+1)\Gamma(n-p+1)}{\Gamma(n+2)\pi}\sin(p+1)\pi \sim \chi\left[\frac{\Gamma(m+1)\Gamma(n-m+1)}{(-1)^{m+1}\Gamma(n+2)}\right]+O(\chi^2) . \quad (17)$$

The asymptotic character for large n of the moments in Eq. (15) is easily determined using Eq. (16) and

$$\frac{(-1)^{m+1}\Gamma(m+1)\Gamma(n-m+1)}{\Gamma(n+2)} \sim \frac{(-1)^{m+1}\Gamma(m+1)}{(n+1)^{m+1}} , \quad (18)$$

which gives moments equivalent to those in Eq. (4). Thus, again, by choosing a slightly different expression for ν_n^{*s} we are able to get exactly the same asymptotic behavior but produce a much simpler form for the singular contribution to the density.

We have found it convenient to label these generalized singularities with the dimensionality of the solid in which they commonly occur. We can easily make an association of the singular behavior produced by the exponent p with the singular behavior characteristic of a $2(p+1)$-dimensional harmonic solid. In Table I we have listed the parameters that produce various singular functions. The sequences of corrections to a particular singular function are listed together. The use of the singular function in Eq. (5) with $p=-1$ and $\epsilon_s=0$ also allows the analysis of δ-function singularities which arise in spatial Fourier transforms of the densities.

Special treatment is needed in dealing with singularities at the ends of the interval, that is, with behavior of $G(x)$ other than proportional to $\sqrt{x(1-x)}$ near $x=0$ or 1. The expansion in Eq. (6) is not appropriate at either $x_s=0$ or $x_s=1$. However, at these points, $\sin(\phi/2)$ in Eq. (5) can be simply written as $\sqrt{x}$ or $\sqrt{1-x}$, respectively. This change requires that the value of p or m must be doubled to produce the corresponding singular dependence at the ends of the interval. For example, the choice of $p=-1$ with $\epsilon_s=+2$ rather than $p=-\frac{1}{2}$ with $\epsilon_s=+1$ provides a one-dimensional minimum at $x_s=0$. The appropriate choices of parameters to produce singularities at the ends of the interval are given in Table II. Note that three-dimensional and higher odd-dimensional "singularities" at the ends of the interval are, in fact, not singularities at all for our choice of orthogonal polynomials. The Chebyshev polynomials of the second kind automatically build in a dependence of $G(x)$ proportional to $[x(1-x)]^{1/2}$ near the ends of the interval. As a consequence, three-dimensional and higher odd-dimensional singularities are automatically incorporated in $G(x)$ and result in no slowly decaying asymptotic behavior in the moments. Of course, if the behavior of the density at the ends of the interval is of the form

$$G(x)\sim x^p(1-x)^q \quad (-1<p,q) , \quad (19)$$

then one solution to removing the singularities at the ends of the interval would be to use as modified moments averages over the appropriate Jacobi polynomials. However, these do not, in general, have the simple interpretation as trigonometric Fourier coefficients that the moments based on Chebyshev polynomials do, and thus reconstruction of additional singularities in the interior of the interval is then more difficult. In addition, if the behavior near the end of the interval is of the form

$$x^p(1+x^q+\cdots) \quad (20)$$

with q not an integer, then even the use of the appropriate Jacobi polynomial will not remove the higher-order singularity. For these reasons we have found it more useful to employ the Chebyshev polynomials and build in the required behavior at the ends of the intervals as described above.

The singular behavior in Eqs. (8) and (14) and the asymptotic contributions to the moments in Eqs. (9) and (15) can be used in Eq. (3) to obtain a very accurate expression for the density of states with the appropriate singular behavior when the singular behavior is known. One way in which the singular behavior can sometimes be determined is through the expansion of the dynamical matrix about a stationary point in the Brillouin zone and subsequent analytic diagonalization to obtain the parameters θ_s, p, ϵ_s, and A_s which determine the location, nature, and amplitude of the singularity. When the locations of the stationary points are unknown, or when the

TABLE I. Parameters defining singular functions at $x_s=\sin^2(\theta_s/2)$ from Eqs. (5) and (12) with $0<x_s<1$ where $\phi=\theta-\theta_s\simeq 0$ and $H(\phi)$ is the Heaviside step function.

Type	Dimension	p or m	ϵ_s	Function
Delta	0	-1	0	$\delta(\phi)$
Minimum	1	$-\frac{1}{2}$	$+1$	
	3	$\frac{1}{2}$	-1	$\lvert\phi\rvert^p H(\phi)$
	5	$\frac{3}{2}$	-3	
	7	$\frac{5}{2}$	$+3$	
Maximum	1	$-\frac{1}{2}$	-1	
	3	$\frac{1}{2}$	$+1$	$\lvert\phi\rvert^p H(-\phi)$
	5	$\frac{3}{2}$	$+3$	
	7	$\frac{5}{2}$	-3	
Minimum	2	0	-2	
	4	1	$+4$	$(\pi/2)\phi^m \operatorname{sgn}\phi$
	6	2	$+2$	
	8	3	0	
Maximum	2	0	$+2$	
	4	1	0	$(\pi/2)\phi^m \operatorname{sgn}(-\phi)$
	6	2	-2	
	8	3	$+4$	
Logarithm	2	0	$+4$	
	4	1	$+2$	$-\phi^m \ln\lvert\phi\rvert$
	6	2	0	
	8	3	-2	
Saddle point ($S1$)	3	$\frac{1}{2}$	$+3$	
	5	$\frac{3}{2}$	$+1$	$-\lvert\phi\rvert^p H(\phi)$
	7	$\frac{5}{2}$	-1	
Saddle point ($S2$)	3	$\frac{1}{2}$	-3	
	5	$\frac{3}{2}$	-1	$-\lvert\phi\rvert^p H(-\phi)$
	7	$\frac{5}{2}$	$+1$	

behavior of the dynamical matrix near the stationary point is too complicated because of a degeneracy, it may not be possible to determine the location, nature, and strength of a singularity in this manner. However, of the most important characteristics of the WPB method and of that developed here is that *the moments themselves can be used to determine the singularities in* $G(x)$. Wheeler, Prais, and Blumstein[3] have very successfully used a differential approximant method proposed by Joyce and Guttmann[8] and refined by Rehr, Joyce, and Guttmann[9] and a nonlinear least-squares method proposed by Golub and Pereyra[10] on the known moments of the density to determine the parameters for the singularities which are not available through the analytic diagonalization of the dynamical matrix. The densities calculated from this moment-singularity method were found to be almost indistinguishable from the exact densities. The same techniques can be used in conjunction with the method developed here.

We have not found any significant differences in the densities calculated using the asymptotic contributions to the moments which are described in this section and those which are described by WPB. The major improvement to the method is the simplified application of the method because the singular behavior of the density is much easier to calculate. The asymptotic contributions to the mo-

TABLE II. Parameters defining singular functions at $x_s=\sin^2(\theta_s/2)$ from Eqs. (5) and (12) with $x_s=0$ and $x_s=1$ where $\phi=\theta-\theta_s\simeq 0$.

Singular functions at $x_s=0$				
Type	Dimension	p or m	ϵ_s	Function
Delta	0	-2	-2	$\delta(\phi)$
Minimum	1	-1	$+2$	$\sqrt{\lvert\phi\rvert^p}\,\mathrm{sgn}\phi$
Minimum	2	0	-2	
	4	2	$+2$	$(\pi/2)\sqrt{\lvert\phi\rvert^p}\,\mathrm{sgn}\phi$
	6	4	-2	
	8	6	$+2$	

Singular functions at $x_s=1$				
Type	Dimension	p or m	ϵ_s	Function
Delta	0	-2	$+2$	$\delta(\phi)$
Minimum	1	-1	-2	$\sqrt{\lvert\phi\rvert^p}\,\mathrm{sgn}(-\phi)$
Maximum	2	0	$+2$	
	4	2	-2	$(\pi/2)\sqrt{\lvert\phi\rvert^p}\,\mathrm{sgn}(-\phi)$
	6	4	$+2$	
	8	6	-2	

ments are simple to calculate and can still be connected to the origin of the singularities in the Brillouin zone.

The use of additional singular corrections provides a good method for the determination of the precise locations of the singularities. The number of known moments which can be fit with the parameters and the existence of other singularities which are not properly fit are the principal limitations of the method.

III. APPLICATIONS

In this section we illustrate the new moment-singularity method with applications to three different densities of states: (1) the density of a linear diatomic chain with $m/M=\frac{1}{2}$, (2) a density consisting of the average of the densities for two diatomic chains, one with $m/M=\frac{1}{2}$, the other with $m/M=\frac{1}{5}$, and (3) the density of states of the two-dimensional triangular lattice with nearest-neighbor interactions. These examples were chosen because they illustrate many challenging features encountered in applications of the method to solids, while at the same time they are either exactly soluble or enough is known about the density that a stringent test of the reliability of the method is possible. In this section we describe the results of the use of differential approximant and nonlinear least-squares methods to identify the singularities in each density. The effects of using various numbers of moments and using various corrections to the singular behavior are described in detail for the calculation of the density of the diatomic chain.

A. Diatomic chain

The density of the diatomic chain provides a good test of the ability of the moment-singularity method because it has a band gap bounded by singularities between which the function should vanish as well as singularities at the ends of the interval where the weight function of the Chebyshev polynomials of the second kind vanishes. The exact density can be written as

$$G(x)=(1/\pi)\left|x-\tfrac{1}{2}\right| \times\left[x(1-x)\left|x-\frac{m}{m+M}\right|\left|x-\frac{M}{m+M}\right|\right]^{-1/2} \tag{21}$$

for $0<x<m/(m+M)$ and $M/(m+M)<x<1$ and is zero elsewhere. The density of the one-dimensional diatomic chain is symmetric about $x=\frac{1}{2}$ with a band gap between a one-dimensional maximum at $x=m/(m+M)$ and a one-dimensional minimum at $x=M/(m+M)$. The density also has one-dimensional extrema at $x=0$ and $x=1$. The Chebyshev modified moments of the first kind for the density with $m/M=\frac{1}{2}$ have been published by Wheeler.[11] In Table III we give the corresponding Chebyshev moments of the second kind calculated by the methods of Ref. 12.

The partial sum to the density of the diatomic chain with $m/M=\frac{1}{2}$ using 20 moments calculated from Chebyshev polynomials of the second kind does not reproduce the singularities at the ends of the interval well. This partial sum is shown in Fig. 3(a). Moments calculated using Chebyshev polynomials of the first kind provide a more recognizable density because the behavior of the

TABLE III. Chebyshev modified moments of the second kind for the diatomic chain with $m/M=\frac{1}{2}$ on the interval $0\le x\le 1$. Odd moments are zero.

n	ν_n^*	n	ν_n^*
0	1.0	26	1.141 567 236 381 853
2	1.222 222 222 222 2222	28	1.032 045 573 376 922
4	0.851 851 851 851 8519	30	1.028 295 977 464 870
6	1.249 657 064 471 879	32	1.136 395 012 219 425
8	0.947 568 968 145 0999	34	0.976 503 460 585 0249
10	1.072 245 084 590 764	36	1.116 672 387 589 492
12	1.138 303 217 102 181	38	1.055 394 731 810 680
14	0.936 781 944 436 6046	40	1.015 444 254 199 506
16	1.175 439 146 689 013	42	1.134 443 425 935 450
18	1.000 688 745 194 373	44	0.991 498 972 347 3244
20	1.046 571 332 587 536	46	1.095 462 703 199 955
22	1.136 250 983 340 722	48	1.073 870 355 076 524
24	0.960 329 038 033 3390		

weighting function $[x(1-x)]^{-1/2}$ mimics the singularities at the ends of the interval. The partial sum using 20 moments calculated with Chebyshev polynomials of the first kind is shown in Fig. 3(b). The use of larger numbers of moments will improve this representation of the density, but the nature and location of the singularities inside the interval (0,1) will still be subject to doubt. While the Chebyshev moments of the first kind fit the singularities at the ends of the interval better, we have used the Chebyshev moments of the second kind for the analysis of all three densities described in this paper to illustrate the ability of the moment-singularity method to fit the singularities at the ends of the interval.

The differential approximant method of Joyce and Guttmann[7] was employed by WPB to identify singularities in the function

$$f(z)=\frac{4}{\pi}\sum_{n=0}^{\infty}\nu_n z^n . \tag{22}$$

Singularities in $f(z)$ on the unit circle $z=e^{i\theta}$ are related to singularities in the density $G(x)$ through the identity[3]

$$G(\sin^2(\theta/2))=\lim_{r\to 1^-}\mathrm{Im}[re^{i\theta}f(re^{i\theta})] . \tag{23}$$

We have found that this method can identify the locations of the dominant singularities in a density when at least six moments are available for each singularity. Thirty moments provide enough information to determine with eight-digit precision the locations of the four singularities in the diatomic chain. Twenty moments determine the locations of the singularities with one or two digits of precision. We have found a strong correlation between the error in the location of the singularity and the distance of the singularity from the unit circle in the complex z plane. This helps eliminate extraneous singularities. We have also found a strong correlation between the error in the value of the exponent and the size of the imaginary part of the exponent. Without good precision in the location of the singularity, however, there is seldom any precision in the value of the exponent. The information about the singularities obtained by this method can then be used in the nonlinear least-squares routine.

The nonlinear least-squares minimization routine of Golub and Pereyra[10] can be used to fit a set of asymptotic contributions from known singularities and their corrections at several locations to a set of known modified moments. We have found that the use of this routine always leads to an accurate determination of the singularities when as few as 20 moments are used and when the initial locations of the singularities at $x_s=\frac{1}{3}$ and $x_s=\frac{2}{3}$ are within 10% of the exact locations. The singularities at $x_s=0$ and $x_s=1$ have been fixed at the ends of the intervals. In Fig. 4(a) we have plotted the density calculated

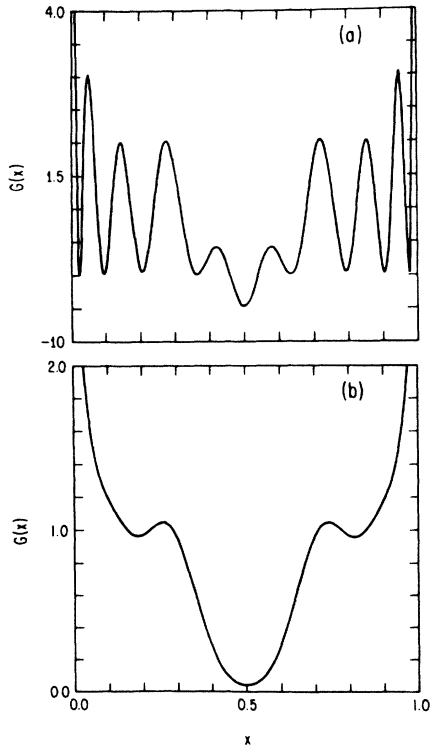

FIG. 3. Partial sum to the density of the diatomic chain with $m/M=\frac{1}{2}$ using (a) 20 Chebyshev moments of the second kind and (b) 20 Chebyshev moments of the first kind.

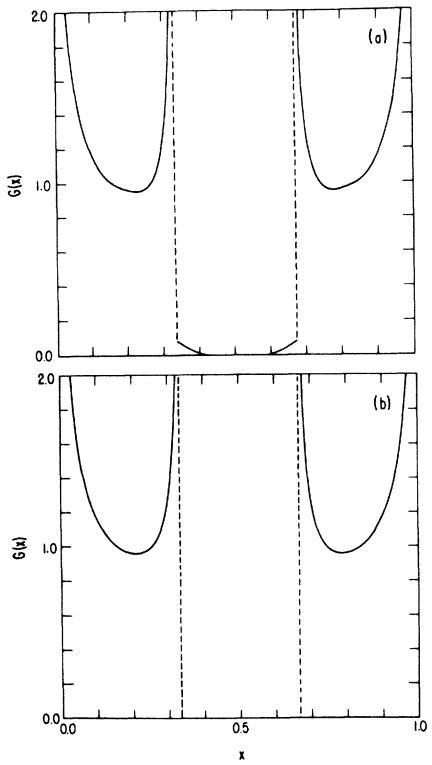

FIG. 4. Density of the diatomic chain with $m/M=\frac{1}{2}$ calculated using 20 Chebyshev moments of the second kind with (a) one-dimensional singular behavior at $x=0$, $x=\frac{1}{3}$, $x=\frac{2}{3}$, and $x=1$ and (b) one-dimensional singularity at $x=0$ and $x=1$ and one-, three-, and five-dimensional singularities at $x=\frac{1}{3}$ and $x=\frac{2}{3}$. (Indistinguishable from exact result on this scale.)

with one-dimensional singularity behavior at $x_s=0$, $x_s=\frac{1}{3}$, $x_s=\frac{2}{3}$, and $x_s=1$ using 20 moments. It is evident that the behavior of the density is fit well.

The use of the additional moments improves the fit of the density at the locations of the singularities and in the band gap. The use of the additional moments dramatically improves the location of the singularities and provides amplitudes in good agreement with the exact amplitudes of the singularities.

The coefficient of $|x_s-x|^p$ in the expansion of the density about the singular point $x=x_s$ within the interval can be compared with the quantity

$$(2/\pi)|A_s|[x_s(1-x_s)]^{-p/2}$$

where $|A_s|$ is the amplitude of the singularity determined by the nonlinear least-squares routine. For $x_s=0,1$ the coefficient of $|x_s-x|^{p/2}$ can be compared to $(2/\pi)|A_s|2^{p+1}$ with the appropriate value of p taken from Table II. Near $x_s=\frac{1}{3}$ the density of the diatomic chain can be expressed as

$$G(x)=(\sqrt{3}/\pi\sqrt{8})y^{-1/2}(1+\tfrac{21}{4}y+\tfrac{27}{32}y^2+\tfrac{3537}{128}y^3+\cdots) \quad (24)$$

in terms of $y=x_s-x>0$. Near $x_s=0$ the density can be written as $G(x)\sim(3/\pi\sqrt{8})x^{-1/2}+\cdots$. The improvements in the locations and coefficients of the one-dimensional singularities at $x_s=0$ and $x_s=\frac{1}{3}$ using larger numbers of moments are shown in Table IV.

The use of additional corrections to the singular behavior of the density also improves the fit of the density. In Table V we show the results of the nonlinear least-squares minimization with as many as three corrections (three, five, and seven dimensional) to the one-dimensional singular behavior at $x_s=\frac{1}{3}$ and $x_s=\frac{2}{3}$ using 20 and 30 moments. The precision in the locations of the singularities increases much more dramatically by adding another correction to the singular behavior than it does by increasing the number of moments from 20 to 30. The calculated amplitudes of the singular behavior are in good agreement with the exact amplitudes, but do not seem to improve with the use of additional corrections. This is also the case when the locations of the singularities are fixed exactly as is shown in Table VI.

Table VII shows a point-by-point comparison of the densities calculated using 20 moments with increasing numbers of corrections to the singular behavior at $x_s=\frac{1}{3}$ and $x_s=\frac{2}{3}$. One-dimensional singularities are included at $x_s=0$ and $x_s=1$. The improvement in the density appears to be less dramatic once we begin to add less singular corrections which appear to have only subtle differences in form. In Table VII we have also included the results of the calculation of the density using the method of Corcoran and Langhoff.[13] This method does very well determining the density without any knowledge of the singularities. However, the moment-singularity method surpasses it because of the incorporation of additional in-

TABLE IV. Locations and coefficients of singularities of the diatomic chain using increasing numbers of Chebyshev moments of the second kind with one-dimensional (1D) singular functions fixed at $x_s=0$ and $x_s=1$ and one-dimensional singular functions floating near $x_s=\frac{1}{3}$ and $x_s=\frac{2}{3}$ in a nonlinear least-squares routine compared with exact values.

Moments	Locations	Singularities	Coefficients
Exact	0.000 000	1D	0.337 619
	0.333 333	1D	0.194 924
50	0.000 000	1D	0.337 591
	0.332 952	1D	0.195 896
40	0.000 000	1D	0.337 566
	0.332 730	1D	0.196 389
30	0.000 000	1D	0.337 503
	0.332 227	1D	0.197 298
20	0.000 000	1D	0.337 287
	0.330 671	1D	0.199 501
10	0.000 000	1D	0.335 587
	0.320 753	1D	0.211 182

TABLE V. Locations and coefficients of singularities of the diatomic chain using Chebyshev moments of the second kind with one-dimensional singular functions fixed at $x_s=0$ and $x_s=1$ and increasing numbers of (coupled) singular functions floating near $x_s=\frac{1}{3}$ and $x_s=\frac{2}{3}$ in a nonlinear least-squares routine compared with exact values.

Moments	Locations	Singularities	Coefficients
Exact	0.000 000	1D	0.337 619
	0.333 333	1D	0.194 924
		3D	1.023 352
		5D	0.164 467
		7D	5.386 304
30	0.000 000	1D	0.337 618
	0.333 325	1D	0.195 540
		3D	1.361 287
		5D	−1.192 046
		7D	4.491 602
30	0.000 000	1D	0.337 617
	0.333 309	1D	0.196 508
		3D	1.011 583
		5D	−1.015 025
30	0.000 000	1D	0.337 614
	0.333 286	1D	0.195 997
		3D	0.990 427
30	0.000 000	1D	0.337 503
	0.332 227	1D	0.197 298
20	0.000 000	1D	0.337 615
	0.333 277	1D	0.195 945
		3D	1.004 492
		5D	−0.659 566
		7D	1.820 318
20	0.000 000	1D	0.337 612
	0.333 231	1D	0.196 100
		3D	0.975 673
		5D	−0.512 465
20	0.000 000	1D	0.337 601
	0.333 143	1D	0.196 640
		3D	0.942 996
20	0.000 000	1D	0.337 287
	0.330 671	1D	0.199 501

TABLE VI. Coefficients of singularities of the diatomic chain using Chebyshev moments of the second kind with one-dimensional singular functions fixed at $x_s=0$ and $x_s=1$ and increasing numbers of (coupled) singular functions fixed at $x_s=\frac{1}{3}$ and $x_s=\frac{2}{3}$ in a nonlinear least-squares routine compared with exact values.

Moments	Locations	Singularities	Coefficients
Exact	0.000 000	1D	0.337 619
	0.333 333	1D	0.194 924
		3D	1.023 352
		5D	0.164 467
		7D	5.386 304
30	0.000 000	1D	0.337 619
	0.333 333	1D	0.195 521
		3D	1.050 871
		5D	−1.227 667
		7D	7.339 251
30	0.000 000	1D	0.337 620
	0.333 333	1D	0.195 514
		3D	1.037 176
		5D	−1.187 726
30	0.000 000	1D	0.337 621
	0.333 333	1D	0.195 911
		3D	1.034 204
30	0.000 000	1D	0.337 796
	0.333 333	1D	0.194 784
20	0.000 000	1D	0.337 620
	0.333 333	1D	0.195 957
		3D	1.045 040
		5D	−0.574 563
		7D	4.658 063
20	0.000 000	1D	0.337 629
	0.333 333	1D	0.195 688
		3D	1.016 400
		5D	−0.846 123
20	0.000 000	1D	0.337 636
	0.333 333	1D	0.196 318
		3D	1.012 289
20	0.000 000	1D	0.338 071
	0.333 333	1D	0.194 465

formation about the singular behavior of the density *determined from the moments themselves.* The density for the diatomic chain calculated from 20 modified moments using the moment-singularity method with one-dimensional singularities at the ends of the interval and one-, three-, and five-dimensional singularities at $x_s=\frac{1}{3}$ and $x_s=\frac{2}{3}$ is shown in Fig. 4(b). This density is superimposable on the exact density except in the very immediate vicinity of the singularities.

B. Superimposed diatomic chains

The average of the densities for diatomic chains with $m/M=\frac{1}{2}$ and $m/M=\frac{1}{5}$ contains the same features as the previously described density plus a one-dimensional maximum within the lower-frequency band at $x_s=\frac{1}{6}$ and a one-dimensional minimum within the higher-frequency band at $x_s=\frac{5}{6}$. The calculation of the moments for this type of density has been described by Wheeler.[11] The Chebyshev moments of the second kind are given in Table VIII. The coefficients of the various singular contributions are given in terms of the expansion of the density:

$$G(x)\sim\frac{3}{2\pi}[(\tfrac{1}{8})^{1/2}+(\tfrac{1}{5})^{1/2}]x^{-1/2} \quad \text{near } x_s=0\,,$$

$$G(x)\sim\frac{1}{2\pi}(\tfrac{6}{5})^{1/2}(x_s-x)^{-1/2} \quad \text{near } x_s=\tfrac{1}{6}\,,$$

$$G(x)\sim\frac{1}{2\pi}(\tfrac{3}{8})^{1/2}(x_s-x)^{-1/2} \quad \text{near } x_s=\tfrac{1}{3}\,.$$

TABLE VII. Point-by-point comparison of the density of the diatomic chain calculated using 20 Chebyshev moments of the second kind with one-dimensional singular functions fixed at $x_s=0$ and $x_s=1$ and increasing numbers of (coupled) singular functions fixed at $x_s=\frac{1}{3}$ and $x_s=\frac{2}{3}$ compared with exact values.

x	1D	1,3D	1,3,5D	1,3,5,7D	Exact	Ref. 13
0.0017	8.202 56	8.199 00	8.198 97	8.198 93	8.198 93	
0.005	4.788 04	4.792 52	4.792 59	4.792 70	4.792 72	5.854 58
0.010	3.395 55	3.401 77	3.401 86	3.401 96	3.401 97	3.259 75
0.020	2.424 37	2.424 52	2.424 51	2.424 49	2.424 49	2.482 78
0.050	1.572 56	1.572 29	1.572 31	1.572 32	1.572 32	1.603 67
0.100	1.170 23	1.167 29	1.167 22	1.167 19	1.167 18	1.159 24
0.150	1.011 30	1.013 65	1.013 74	1.013 74	1.013 76	1.007 66
0.300	1.231 42	1.254 84	1.255 62	1.255 87	1.256 60	1.221 88
0.330	3.437 63	3.446 64	3.439 95	3.442 60	3.435 30	2.976 93
0.3317	4.876 69	4.886 37	4.874 84	4.879 18	4.864 49	2.642 28
0.3333	33.7049	34.0033	33.8979	33.9414	33.7678	2.254 65
0.335	0.061 09	−0.007 51	−0.003 97	−0.007 05	0.0	1.755 49
0.340	0.051 61	−0.004 79	−0.001 79	−0.004 29	0.0	0.731 18
0.350	0.032 22	−0.002 57	−0.000 52	−0.002 06	0.0	0.142 14
0.400	0.013 10	0.000 19	−0.000 10	0.000 20	0.0	0.001 21
0.450	−0.001 50	0.000 14	−0.000 01	0.000 06	0.0	
0.500	0.008 32	−0.000 20	0.000 08	−0.000 18	0.0	

These coefficients are compared to those obtained from the nonlinear least-squares method in Table IX. The averaged density for diatomic chains calculated using 30 moments and the moment-singularity method with one-dimensional singularities at the ends of the interval and one-, three-, and five-dimensional singularities at $x_s=\frac{1}{6}$, $x_s=\frac{1}{3}$, $x_s=\frac{2}{3}$, and $x_s=\frac{5}{6}$ is shown in Fig. 5. This density is again superimposable on the exact density except in the vicinity of the singularities. The fit of this density is slightly poorer than the previous one near the singularities because there are more singularities to fit with the same number of moments. Even so, the fitting of this density shows that the moment-singularity method is able to fit a density with a band gap and singularities within the bands with very good precision.

C. Two-dimensional triangular lattice

The exact dispersion relation and an approximate density for the nearest-neighbor two-dimensional triangular lattice were calculated by Dean.[14] The density has logarithmic singularities within the interval and discontinuities at the ends of the interval, that is, $G(x)$ approaches a constant at $x=0$ and $x=1$. In addition to these singularities exhibited by Dean's calculation, our moment-singularity

TABLE VIII. Chebyshev modified moments of the second kind for the superimposed densities of a diatomic chain with $m/M=\frac{1}{2}$ and a diatomic chain with $m/M=\frac{1}{5}$ on the interval $0\le x\le 1$. Odd moments are zero.

n	ν_n^*
0	1.0
2	1.555 555 555 555 555
4	1.074 074 074 074 074
6	1.113 854 595 336 076
8	1.209 114 464 258 497
10	1.337 905 807 041 609
12	1.155 475 396 139 928
14	1.045 875 898 422 088
16	1.353 586 234 826 107
18	1.233 069 999 041 789
20	1.094 767 246 837 868
22	1.204 551 501 414 533
24	1.249 669 239 452 023
26	1.251 676 138 955 587
28	1.092 963 950 056 062

TABLE IX. Locations and coefficients of the dominant singular contributions of the superimposed densities of two diatomic chains using 30 Chebyshev moments of the second kind with one-dimensional (1D) singular functions fixed at $x_s=0$ and $x_s=1$ and one-, three-, and five-dimensional singular functions near $x_s=\frac{1}{6}$, $x_s=\frac{1}{3}$, $x_s=\frac{2}{3}$, and $x_s=\frac{5}{6}$ in a nonlinear least-squares routine compared with exact values.

Moments	Locations	Singularities	Coefficients
Exact	0.000 000	1D	0.382 338
	0.166 667	1D	0.174 346
	0.333 333	1D	0.097 462
30	0.000 000	1D	0.382 337
	0.166 639	1D	0.174 786
	0.333 331	1D	0.097 729
20	0.000 000	1D	0.382 345
	0.166 189	1D	0.171 807
	0.331 529	1D	0.101 811

TABLE X. Chebyshev modified moments of the second kind for the density of the two-dimensional triangular lattice on the interval $0 \leq x \leq 1$.

n	ν_n^*
0	1.0
1	0.0
2	0.333 333 333 333 3333
3	−0.222 222 222 222 2222
4	0.111 111 111 111 1111
5	0.148 148 148 148 1481
6	0.102 880 658 436 2140
7	−0.246 913 580 246 9138
8	0.781 893 004 115 2267
9	−0.908 398 110 044 2011
10	0.155 311 690 291 1142
11	0.354 620 738 708 5295
12	0.116 005 351 487 7486
13	−0.196 447 018 577 7982
14	0.236 470 276 098 3831
15	0.284 384 030 086 7422
16	0.111 675 614 038 0590
17	−0.396 582 122 944 9751
18	0.239 733 087 529 0926
19	−0.385 486 581 738 3356
20	0.309 864 071 231 4028
21	0.379 384 684 530 7129
22	0.327 484 254 453 0498
23	−0.390 891 716 622 6604
24	0.409 739 280 005 4602
25	0.833 653 035 492 0710
26	0.528 442 902 713 3334
27	0.967 158 622 930 1810
28	−0.560 309 955 949 2450
29	−0.307 237 179 645 6187

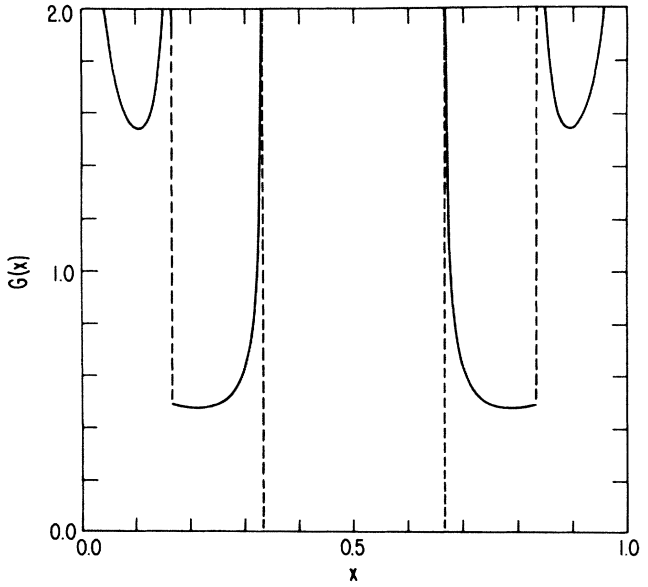

FIG. 5. Superimposed densities of the diatomic chain with $m/M = \frac{1}{2}$ and of the diatomic chain with $m/M = \frac{1}{5}$ calculated using 30 Chebyshev moments of the second kind with one-dimensional singularities at $x = 0$ and $x = 1$ and one-, three-, and five-dimensional singularities at $x = \frac{1}{6}$, $x = \frac{1}{3}$, $x = \frac{2}{3}$, and $x = \frac{5}{6}$. (Indistinguishable from exact result on this scale.)

TABLE XI. Locations and coefficients of dominant singular contributions of the two-dimensional triangular lattice calculated using 30 Chebyshev moments of the second kind with two-, four-, and six-dimensional singular functions fixed at $x_s = 0$ and $x_s = 1$; with two-, four-, and six-dimensional singular functions floating near $x_s = \frac{1}{3}$ and $x_s = \frac{27}{32}$; and with four- and six-dimensional singular functions floating near $x_s = \frac{3}{4}$ compared with exact values.

Moments	Locations	Singularities	Coefficients
Exact	0.000 000	2D	0.735 105
	0.333 333	2D	0.344 662
	0.750 000	4D	2.940 421
	0.843 750	2D	
	1.000 000	2D	0.954 930
50	0.000 000	2D	0.735 002
	0.333 330	2D	0.344 738
	0.750 200	4D	2.816 622
	0.843 753	2D	0.353 654
	1.000 000	2D	0.954 728
40	0.000 000	2D	0.735 208
	0.333 331	2D	0.344 531
	0.750 601	4D	2.781 383
	0.843 745	2D	0.354 770
	1.000 000	2D	0.955 250
30	0.000 000	2D	0.734 904
	0.333 328	2D	0.345 004
	0.751 792	4D	2.726 460
	0.843 934	2D	0.354 952
	1.000 000	2D	0.953 262
20	0.000 000	2D	0.732 766
	0.333 129	2D	0.342 620
	0.768 701	2D	4.914 690
	0.847 406	2D	0.314 259
	1.000 000	2D	0.946 292

method suggested the existence of a discontinuity in slope at $x_s = \frac{3}{4}$. This omission by Dean was undoubtedly simply due to the approximate nature of his calculation. The density calculated using 30 Chebyshev modified moments of the second kind and our moment-singularity method with two-, four-, and six-dimensional singularities at $x_s = 0$, $x_s = \frac{1}{3}$, $x_s = \frac{27}{32}$, and $x_s = 1$ and with four- and six-dimensional singularities at $x_s = \frac{3}{4}$ is shown in Fig. 6. The moments, calculated exactly using the Brillouin-zone sampling technique of Isenberg[15] in conjunction with the recursive product-trace method of Wheeler and Blumstein,[5] are given in Table X. Subsequent to fitting the density using the moment-singularity method, we analyzed the two-dimensional Brillouin zone to determine the exact locations of all singularities and the amplitudes of all singularities except the one at $x_s = \frac{27}{32}$.[16] The comparison between the exact coefficients and the coefficients calculated with the moment-singularity method is shown in Table XI. The logarithmic singularities in the density arise from two-dimensional saddle points in the dispersion relation and the discontinuities arise from two-

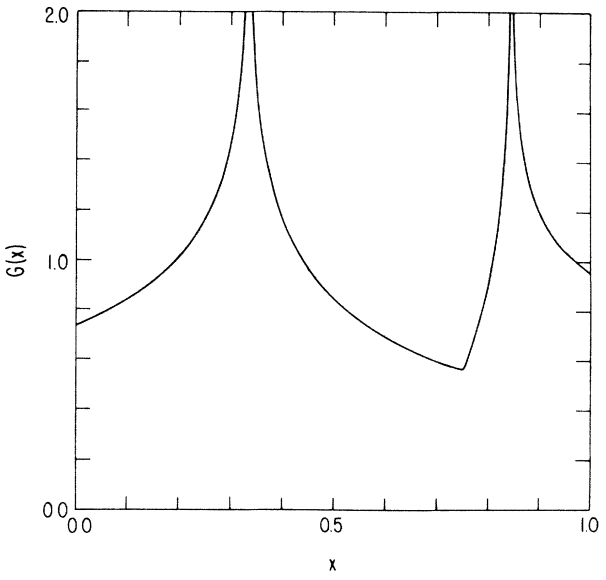

FIG. 6. Density of two-dimensional triangular lattice calculated using 30 Chebyshev moments of the second kind with two-, four-, and six-dimensional singularities at $x=0$, $x=\frac{1}{3}$, $x=\frac{27}{32}$, and $x=1$ and four- and six-dimensional singularities at $x=\frac{3}{4}$. (Indistinguishable from exact results on this scale.)

dimensional extrema. The discontinuity in slope at $x_s=\frac{3}{4}$ which is characteristic of singularities found in four-dimensional solids arises from a cone-shaped crossover of two bands of frequencies at the corners of the hexagonal Brillouin zone. A more recent root sampling calculation of the density by Hoover[17] does show evidence for the discontinuity in slope at $x_s=\frac{3}{4}$.

IV. CONCLUSION

Improvements have been made in the moment-singularity method by simplifying the functional form of the singular behavior which is used to fit the density of states. The improved method also provides a prescription for the use of less singular corrections to the determined singular behavior. The use of additional corrections in the nonlinear least-squares method described in Sec. III provides a method to precisely determine the locations of singularities in the density.

The moment-singularity method is able to provide information about singularities within bands, at band edges, and at the ends of the intervals over which densities are defined. In addition, this method provides such compelling information about singularities that are not expected to appear in densities that a two-dimensional singularity (a discontinuity at $x=0.05$) was found by WPB in the density of a three-dimensional fcc lattice and that a four-dimensional singularity (a discontinuity in slope at $x=\frac{27}{32}$) was found in the two-dimensional triangular lattice described here.

The improvements in the moment-singularity method described here retain the precision of the earlier method of WPB. While the method of Corcoran and Langhoff probably provides the most accurate purely mechanical method of calculating a density from its moments, the moment-singularity method is shown to outperform it if, in addition, one is willing to analyze the information present in the moments and to build the appropriate singular functions into the density. It should be emphasized that each of these methods uses only the moments generated from the interaction matrix of the lattice to calculate the density. It seems likely that each of these methods will find its uses. The method of Corcoran and Langhoff has the advantage of being purely mechanical and thus not subject to the interpretation of individual investigators. The moment-singularity method has the advantage of greater potential for the analysis and incorporation of singularities in the density from the moments. In addition, the density of Corcoran and Langhoff reproduces the known moments only approximately, while that of the moment-singularity method reproduces the known moments exactly.

ACKNOWLEDGMENTS

This research was supported by the National Science Foundation through Grants Nos. CHE 75-20624, CHE 79-2518, and CHB 81-19247. Helpful conversations with William Hoover are gratefully acknowledged.

*Permanent address: Chemistry Department, Roosevelt University, Chicago, IL 60605.

[1]M. Lax and J. L. Lebowitz, Phys. Rev. **96**, 594 (1954).
[2]H. B. Rosenstock, Phys. Rev. **97**, 290 (1955).
[3]J. C. Wheeler, M. G. Prais, and C. Blumstein, Phys. Rev. B **10**, 2429 (1974).
[4]R. A. Sack and A. F. Donovan, Numer. Math. **18**, 465 (1972).
[5]J. C. Wheeler and C. Blumstein, Phys. Rev. B **6**, 4380 (1972).
[6]In these cases the moments can be expressed as a multiple integral over reciprocal space $\nu_n^* \sim \int d\mathbf{k} \sin(n+1)\theta(\mathbf{k})$ which for large n is dominated by the stationary point $\theta_s=\theta(\mathbf{k}_s)$ and is evaluated by standard asymptotic methods. See, for example, A. Erdeleyi, *Asymptotic Expansions* (Dover, New York, 1956), p. 51ff.
[7]M. G. Prais and J. C. Wheeler (unpublished).
[8]G. S. Joyce and A. J. Guttman, in *Padé Approximants and their Applications* (Academic, New York, 1973), pp. 163–168.
[9]J. J. Rehr, G. S. Joyce, and A. J. Guttmann, J. Phys. A **13**, 1587 (1980).
[10]G. H. Golub and V. Pereyra, SIAM J. Numer. Anal. **10**, 413 (1973).
[11]J. C. Wheeler, J. Chem. Phys. **80**, 472 (1984).
[12]C. Blumstein and J. C. Wheeler, Phys. Rev. B **8**, 1764 (1973).
[13]C. T. Corcoran and P. W. Langhoff, J. Math. Phys. **18**, 651 (1977).
[14]P. Dean, Proc. Philos. Soc. **59**, 383 (1963).
[15]C. Isenberg, Phys. Rev. **132**, 2427 (1963).
[16]The amplitude of the logarithmic singularity at $x_s=\frac{27}{32}$ was

not determined because the singularity arises from a yet to be located stationary point in the Brillouin zone with less than maximal symmetry. The discontinuity in slope at $x_s = \frac{3}{4}$ arises from the simultaneous vanishing of the gradient of the regular contribution to $\omega(\mathbf{k})$ and of the argument of the square-root contribution to $\omega(\mathbf{k})$ in the dispersion relation given by Dean (Ref. 14). This leads to a "conelike" variation in frequency with wave vector.

[17]W. G. Hoover, A. J. C. Ladd, and N. E. Hoover, in *Interatomic Potentials and Crystalline Defects,* edited by J. K. Lee (American Institute of Mechanical Engineers, 1981), p. 273.